Chemical Science

Accepted Manuscript

This article can be cited before page numbers have been issued, to do this please use: C. F. Chow, P. Ho, W. Wong, Y. Lu, Q. Tang and C. Gong, *Chem. Sci.*, 2017, DOI: 10.1039/C6SC05584B.

ROYAL SOCIETY OF CHEMISTRY

rsc.li/chemical-science

View Article Online
DOI: 10.1039/C6SC05584B

Catalyst Displacement Assay: A Supramolecular Approach for the Design of Smart Latent Catalysts for Pollutant Monitoring and Removal

Cheuk-Fai Chow,*[a] Pui-Yu Ho,[b] Wing-Leung Wong,*[b] Yu-Jing Lu,[c] Qian Tang[a] and Cheng-Bin Gong,*[a]

[a] Department of Science and Environmental Studies, The Education University of Hong Kong, 10 Lo Ping Road, Tai Po Hong Kong SAR, China and College of Chemistry and Chemical Engineering, Southwest University, Chong Qing, China

[b] Centre for Education in Environmental Sustainability, The Education University of Hong Kong, 10 Lo Ping Road, Tai Po, Hong Kong SAR, China.

[c] Institute of Natural Medicine and Green Chemistry, School of Chemical Engineering and Light Industry, Guangdong University of Technology, Guangzhou 510006, P.R. China.

E-mail: cfchow@ied.edu.hk; Fax: (+852) 29487676; Tel: (+852) 29487671

Abstract:

Latent catalysts can be tuned to function smartly by assigning a sensing threshold using the displacement approach for targeted analytes. Three cyano-bridged bimetallic complexes were synthesized as "smart" latent catalysts by the supramolecular assembly of different metallic donors ($[Fe^{II}(CN)_6]^{4-}$, $[Fe^{II}(t\text{Bubpy})(CN)_4]^{2-}$, and $Fe^{II}(t\text{Bubpy})_2(CN)_2$ with a metallic acceptor $[Cu^{II}(dien)]^{2+}$. The investigation of both their thermodynamic and kinetic properties on binding with toxic pollutants provided insight into their smart off-on catalytic capabilities, enabling us to establish a threshold-controlled catalytic system for the degradation of pollutants such as cyanide and oxalate. With these smart latent catalysts, a

new catalyst displacement assay (CDA) was demonstrated and applied in a real wastewater treatment process to degrade cyanide pollutants in both domestic (level I, untreated) and industrial wastewater samples collected in Hong Kong, China. The smart system was smartly adjusted to able to initiate the catalytic oxidation of cyanide at a threshold concentration of 20 μM (the World Health Organization's suggested maximum allowable level for cyanide in wastewater) to the less harmful cyanate under ambient conditions.

Introduction

The development of "smart" catalysts for process monitoring and reaction control is highly important in modern chemistry. In particular, a smart catalyst that is able to execute a specific task under certain conditions would be very attractive. Different from traditional catalysts that initiate a reaction once the reactants are present, this type of catalyst would provide extra benefits for certain industrial processes such as contaminant removal during water treatment. Traditionally, chemists have focused on catalyst use to increase rates, yields, and/or the stereo-selectivity of reactions.[1] However, it is possible that catalysts could be made "smarter" with the incorporation of extra control parameters, such as introducing an analyte-selective receptor which is also an inhibitor of the catalyst, so that the catalyst can only function when a specific analyte exists under certain conditions. This sort of smart catalyst is rarely found in the literature, although it could be rationally designed to associate with an inhibitor and be temporarily deactivated, but readily re-activated in the presence of a specific trigger or an initiator to start the targeted reaction under given conditions such as concentration, temperature, or pH. Recently, several catalytic systems demonstrated a portion of this "smart off-on" function for controlling targeted reactions, which led to very interesting reaction outcomes.[2] A switch-based negative feedback loop demonstrated with a zinc(II) ion coordination-coupled deprotonation of a hydrazine is a typical example of smart control system, in which a particular threshold of zinc(II) causes the releasing of certain

concentration of protons to the environment to trigger a cascade of reactions.[2j] Based on these ideas, we conjectured that a further advancement of the "off-on" approach would be the introduction of a threshold-controlled function into the catalysts. The advancement demonstrated in this study overcomes the limitations of simple "catalyst-inhibitor" systems, arising from their simple off-on designs: i.e., they lack a mechanism to control the initiation threshold, so that the catalytic reaction will ensue in the presence of small amounts of initiator without having reached a specific initiator threshold.

The catalyst displacement assay (CDA) is a useful protocol for developing smart latent catalytic systems, particularly in chemical or waste treatment applications, because chemical toxicity depends on dosage. For example, cyanide (CN^-) is well known for its high toxicity and has been identified as one of the most serious threats toward the environment and human life. Nevertheless, it is widely used in gold mining, electroplating, and the production of synthetic fibers.[3] Considering its industrial importance as well as its adverse effects, the World Health Organization has suggested maximum allowable levels of cyanide in wastewater, fresh water (class III), and drinking water of 0.5, 0.2, and 0.05 $mg \cdot L^{-1}$, respectively.[4] The elimination of cyanide is therefore only sensible when its levels exceed these thresholds. The removal of cyanide in aqueous solution by oxidation has been well studied with oxidants in presence of various catalysts such as TiO_2,[5] Cu(I)/Cu(II) transition metal complexes[6] and Fe(II)-Cu(II) bimetallic complex[18a]. Nonetheless, these systems are not "smart" enough to begin functioning under a specific set of conditions. In recent years, the molecular design and synthesis of chemosensing systems specifically for cyanide recognition or determination have been reported.[7a–d] Some of these molecular systems are indicator displacement assays (IDA), which show sensing properties with good selectivity and signal changes upon binding with CN^- in solution.[7e–j] IDA involves the specific analyte competition, which causes the displacement of the indicator from the

receptor and gives off-on signals. The advantage of an IDA system is that the selectivity and sensitivity can be adjusted by tuning the thermodynamics of the ensemble. A number of IDA sensing systems[8–11] are well-established for the determination of anions,[8a–b,9a–b,10a–e,11b-c] neutral organic molecules,[11d-e] zwitterions,[8c–d,9c–d,11a] and other molecules;[8e] however, there are no examples of IDA systems showing smart properties that can effect a catalytic reaction under pre-set conditions.

On the basis of IDA systems, we attempted to establish a CDA system based on supramolecular donor-acceptor complexes which would feature a smart system that could selectively recognize a target analyte (a pollutant like CN^-), after which a pre-set catalytic reaction would be automatically performed under given conditions. With the new CDA system design, the catalyst is controllably activated when the analyte level reaches a certain threshold to start a catalytic reaction. In this study, we demonstrate that a threshold and the off/on control parameter can be rationally adjusted by understanding the thermodynamic and kinetic properties of cleavage processes in the donor-acceptor complexes. Both thermodynamic and kinetic characteristics are the crucial factors in deriving a CDA system that could generate a number of advantages for chemical processes—including the reduced or minimized use of reagents, costly catalysts, energy, and manpower—which cannot be provided by traditional chemical reactions or catalytic systems.

Experimental Section

Materials and general procedures. 4,4′-Di-*tert*-butyl-2,2′- bipyridine (*t*Bubpy), diethylenetriamine (dien), $K_4[Fe(CN)_6]$, potassium oxalate, and potassium cyanide were obtained from Aldrich. Complexes $K_2[Fe^{II}(tBubpy)(CN)_4]$,[12] $Fe^{II}(tBubpy)_2(CN)_2$,[13] and $Cu^{II}(dien)Cl_2$[14] were prepared according to reported methods.

View Article Online
DOI: 10.1039/C6SC05584B

Physical measurements and instrumentation. Electrospray ionization mass spectrometry (ESI-MS) was performed using an AB SCIEX API 2000 LC/MS/MS system. Elemental analyses were conducted using a Vario EL CHN analyzer. Infrared spectra in the 500–4000 cm^{-1} range using KBr pellets were recorded using a Perkin Elmer Model Frontier FTIR spectrometer, and UV-vis spectra were measured on a Cary 50 ultraviolet-visible spectrophotometer. Dissolved organic carbon was recorded using a Shimadzu TOC-L CSH High-Sensitivity Total organic Analyzer. The emission spectra were recorded using a Horiba FluoroMax-4 spectrofluorimetric with a 5 nm slit width and a 0.5 s integration time. Broad-band UV irradiation was provide by 500W Hg(Xe) light source (Model 66485) with a digital power supply system (Model 69911) by Newport Inc.

UV-vis spectroscopic titrations. The analytical grade DMF used in the UV-vis spectroscopic titrations was purified by distillation. The titrations of $K_4[Fe^{II}(CN)_6]$ (3.3×10^{-4} M) by $Cu^{II}(dien)Cl_2$ (0 to 2×10^{-5} M) were conducted in HEPES buffer at pH 7.4. While the titrations of $K_2[Fe^{II}(^tBubpy)(CN)_4]$ (5×10^{-5} M) by $Cu^{II}(dien)Cl_2$ (0 to 2×10^{-4} M) and $Fe^{II}(^tBubpy)_2(CN)_2$ (5×10^{-5} M) by $Cu^{II}(dien)Cl_2$ (0 to 1×10^{-4} M) were carried out in a mixture of aqueous HEPES buffer (1.50 mL, pH 7.4) with DMF(1.50 mL). UV–vis spectroscopic titrations of $Cu^{II}(dien)Cl_2$ (5×10^{-4} M) with oxalate (0 to 1×10^{-3} M) were carried out in aqueous phosphate buffer pH 4. All measurements were taken after standing for 12 h to ensure their equilibria were reached. Binding constants (log *K*) and formation energies (ΔG/kJ mol^{-1}) were analyzed according to the Benesi–Hildebrand equations[15-16] from the UV-vis spectroscopic titrations.

Kinetic measurements: **Cleavage of cyano-bridges between the Fe^{II} and Cu^{II} metal centers of 1–3 by cyanide.** The experimental procedure for the rate constant measurements

View Article Online
DOI: 10.1039/C6SC05584B

was performed according to previous studies.[17] Except complex **1** in pH 7.4 HEPES buffer, all reactions were performed in DMF/pH 7.4 HEPES buffer (1:1 v/v). By mixing a known amount of cyanide solution (2.5×10^{-3} to 1.25×10^{-2} M) with the test solutions at 25 °C containing 2.5×10^{-4} M complex, the changes in the absorbance due to the addition of cyanide were measured at different time intervals. All kinetics measurements were conducted under ambient conditions.

Oxidation of cyanide to cyanate with complexes 1–3 as catalysts. All experiments were conducted in a 40 mL boiling tube in the absence of light, and the test solutions (15.0 mL) were stirred during the experiments. The concentration of H_2O_2 was 6.53 mM, and the concentrations of complexes **1, 2,** and **3** were 0.1, 0.1, and 0.2 mM, respectively. Different initial concentrations of cyanide (0 to 1000 μM) were used in the studies. The concentrations of CN^- and NCO^- in the test solutions were measured at regular intervals using previously reported analytical methods.[18a]

Photocatalytic degradation of oxalate to CO_2 by complex 1 as catalyst. All experiments were conducted in a 50.0 mL volumetric flask with a 500 W Hg(Xe) ultraviolet–visible lamp (Newport) irradiation source. The experimental setup was completely shielded from surrounding light. The distance between the lamp and test solution was about 25 cm. A water bath was placed between the lamp and test solution to absorb heat generated by the UV irradiation. Prior to irradiation, the pH of the test solution was adjusted to 1.5 with HCl/KCl buffer. Generally, during the photocatalytic experiments, a test solution (50.0 mL) containing complex **1** (6.25×10^{-4} M) and H_2O_2 (0.4 M) was irradiated while the oxalate concentration was varied from 6.25×10^{-4} to 3.125×10^{-2} M. The dissolved organic carbon (DOC) in the system was determined at regular intervals to evaluate catalytic efficiency.[18b]

View Article Online
DOI: 10.1039/C6SC05584B

Synthesis and characterization

$[Fe^{II}(CN)_6]$–$[Cu^{II}(dien)(H_2O)]_2$ (1). The complex was synthesized by modification of the reported method.[19] A mixture of $K_4[Fe^{II}(CN)_6]$ (1.00 g, 2.37 mmol) and $Cu^{II}(dien)Cl_2$ (0.56 g, 2.37 mmol) was stirred in a water/methanol mixture (1:1 v/v, 25 mL) at room temperature overnight. The green precipitate obtained by filtration was washed with deionized (DI) water and acetone, and then air-dried. Yield: 0.54 g (84.5%). IR (KBr): $\nu_{C\equiv N}$ = 2039, 2047, 2103 cm^{-1}. ESI-MS (MeOH, +ve mode): *m/z* 544.8 $\{[Fe(CN)_6][Cu^{II}(dien)]_2\}H^+$ (mass = 545.0 g mol^{-1}; charge = +1); elemental analysis calcd (%) for $C_{14}Cu_2FeH_{26}N_{12}\cdot 4H_2O$ (**1**): C 27.23; H 5.55; N 27.22; found: C 27.29; H 5.52; N 26.95.

$[Fe^{II}(t\text{Bubpy})(CN)_4]$–$[Cu^{II}(dien)Cl]_2$ (2). The complex was synthesized following the reported method.[18] A mixture of $K_2[Fe(t\text{Bubpy})(CN)_4]$ (0.115 g, 0.2 mmol) and $Cu^{II}(dien)Cl_2$ (0.05 g, 0.2 mmol) was stirred in a water/methanol mixture (1:1 v/v, 5 mL) at room temperature overnight. The brown precipitate obtained upon centrifugation was washed with DI water and acetone, and then air-dried. Yield: 0.069 g (83.1%). IR (KBr): $\nu_{C\equiv N}$ = 2059, 2084, 2103, 2114 cm^{-1}. ESI-MS (MeCN, +ve mode): *m/z* 380.1 $\{Fe(t\text{Bubpy})(CN)_4[Cu^{II}(dien)]_2\}^{2+}$ (mass = 760.2 g mol^{-1}; charge = +2); elemental analysis calcd (%) for $C_{30}Cl_2Cu_2FeH_{50}N_{12}$ **(2)**: C 43.27; H 6.05; N 20.19; found: C 43.22; H 6.10; N 20.10.

$\{[Fe^{II}(t\text{Bubpy})_2(CN)_2]_2$–$[Cu^{II}(dien)]\}Cl_2$ (3). A mixture of $Fe^{II}(t\text{Bubpy})_2(CN)_2$ (0.10 g, 0.16 mmol) and $Cu^{II}(dien)Cl_2$ (0.038 g, 0.16 mmol) was stirred in methanol (25 mL) at room temperature overnight. The reddish brown solid obtained after evaporation was washed with chloroform, DI water, and acetone, and then air-dried. Yield: 0.0745 g

(61.1%). IR (KBr): $\nu_{C\equiv N}$ = 2068, 2082 cm^{-1}. ESI-MS (MeOH, +ve mode): *m/z* 726.9 $\{[Fe(t\text{Bubpy})_2(CN)_2]_2Cu^{II}(dien)\}^{2+}$ (mass = 1454.70 g mol^{-1}; charge = +2); elemental analysis calcd (%) for $C_{80}Cl_2Cu_1Fe_2H_{109}N_{15}\cdot CH_3C(O)CH_3$ **(3)**: C 62.81; H 7.62; N 11.94; found: C 63.52; H 7.62; N 11.73.

Results and Discussion

Syntheses of bimetallic complexes 1–3. Metallic donors (M_D) coordinated with a bridging ligand such as the commonly used $^-$CN, $^-$NCS, or $^-$NCO ligands are able to bond with a metallic acceptor (M_A) to form a desirable bimetallic complex of the form M_D–bridge–M_A. Through this supramolecular assembly, bimetallic complexes can be designed to achieve desired functionalities which are not offered by the individual mono-metallic precursors (M_D or M_A). We studied a series of bimetallic complexes containing a cyano-bridge, M_D–C≡N–M_A, where M_D = Re^I, Fe^{II}, Ru^{II}, or Os^{II}; and M_A = Ni^{II}, Cu^{II}, Pt^{II}, or Ln^{III}.[11] Interestingly, the strength of the bridging bond between the metal centers is adjustable and depends on the combination of M_D and M_A. Therefore, by regulating the two metal centers connected by the cyano-bridge, a bimetallic complex with specific functionality can be tailored. In this study, M_D, functioning as an inhibitor, was introduced into a catalyst M_A to generate a CDA system with an "off-on" function in which a catalytic oxidation reaction could be triggered when a certain concentration of cyanide ion was present in the solution. The influence of the thermodynamic and kinetic properties of the cyano-bridges of the bimetallic complexes on the control of the off-on and threshold operation of the catalyst was then illustrated comprehensively.

Bimetallic complexes **1–3** shown in Scheme 1 were synthesized with the metallic acceptor $Cu^{II}(dien)Cl_2$ and the latent catalyst donors $K_4[Fe(CN)_6]$, $K_2[Fe^{II}(t\text{Bubpy})(CN)_4]$, and $Fe(t\text{Bubpy})_2(CN)_2$. All three bimetallic complexes were isolated as air-stable solids and

View Article Online
DOI: 10.1039/C6SC05584B

were characterized by IR spectroscopy, electrospray ionization mass spectrometry (ESI-MS), and elementary CHN analysis. The three cyano-ferrous complexes, $K_4[Fe^{II}(CN)_6]$, $K_2[Fe^{II}(t\text{Bubpy})(CN)_4]$, and $Fe^{II}(t\text{Bubpy})_2(CN)_2$, were designed systematically as the M_D species because they are able to participate in coordinating cyano bridging with other metal complexes to form bimetallic complexes, whereas $[Cu^{II}(\text{dien})]Cl_2$ was selected as the model acceptor M_A because it can catalyze the oxidation of organic/inorganic pollutants such as oxalate and cyanide ions. We expected the strengths of the cyano-bridges of the three bimetallic complexes to be different due to the variation of the charge densities among the ferrous M_D from −4, −2, to 0. The cyano bridge activities of the bimetallic complexes **1–3** significantly impact their thermodynamics and kinetics, which are considered as the determinant for the threshold of a smart catalytic system.

The formation of cyano-bridges between the M_D and M_A units in the bimetallic complexes was confirmed by IR spectroscopy, as shown in Table 1. In general, all the $\nu_{C\equiv N}$ stretching frequencies observed in **1–3** are red shifted with respect to their precursor cyano-ferrous complexes, and the degrees of the shift vary by 2, 29, and 60 cm^{-1}, respectively. These changes can be attributed to the electron density differences among the M_D complexes, $Fe^{II}(\text{tBubpy})_2(CN)_2$, $[Fe^{II}(\text{tBubpy})(CN)_4]^{2-}$, and $[Fe^{II}(CN)_6]^{4-}$.

In the bimetallic complex syntheses, 1:1 molar ratios of the Fe^{II} and Cu^{II} starting materials were used in all cases. Interestingly, however, the compositions of supramolecular structures **1–3** contained Fe^{II}/Cu^{II} ratios of 1:2, 1:2, and 2:1, as verified by ESI-MS, spectroscopic titration studies, and CHN elemental analysis. As shown in Figure 1, **1–3** show peaks at *m/z* = 544.8, 380.1, and 726.9, representing $\{[Fe^{II}(CN)_6]–[Cu^{II}(\text{dien})]_2\}H^+$, $\{[Fe^{II}(t\text{Bubpy})(CN)_4]–[Cu^{II}(\text{dien})]_2\}^{2+}$, and $\{[Fe^{II}(t\text{Bubpy})_2(CN)_2]_2–[Cu^{II}(\text{dien})]\}^{2+}$, respectively. The elemental analysis results for **1–3** also matched the proposed structures. In

addition, the binding isotherms (Figures S1–S3, Supporting Information (SI)) obtained by the titration of $Cu^{II}(dien)Cl_2$ solution with $K_4[Fe^{II}(CN)_6]$, $K_2[Fe^{II}(t\text{Bubpy})(CN)_4]$, and $Fe^{II}(t\text{Bubpy})_2(CN)_2$, respectively, show that the bimetallic complexes **1–3** formed in the solution in the above Fe^{II}/Cu^{II} ratios.[15]

Thermodynamic and kinetic investigations of the CDA system. In the design of a CDA, a catalyst should first be bound temporarily to an inhibitor. Cu^{II} complexes have been well studied as active catalysts for the oxidation of cyanide using H_2O_2 as the oxidant.[18a,20] However, the catalytic activity is inhibited when the Cu^{II}-centers are bridged to Fe^{II}-centers with a ligand (C≡N) in the form of bimetallic complexes.[18a] The Cu-catalyst at this stage is de-activated as it is bridging with its metallic counterpart. When a competitive analyte, i.e., the reactant, is introduced into the system, it causes the displacement of the catalyst from the inhibitor, thus freeing it.[18a] At this stage, the Cu-catalyst is activated to execute its catalytic function under the given conditions. For the present CDA system ($[(L)_x(CN)_yFe^{II}$—C≡N—$Cu^{II}(dien)]$, Scheme 2), the study of the coordination with cyano-bridges between the Fe^{II} and Cu^{II} metal centers allows us to understand the thermodynamic and kinetic properties of these bimetallic systems. These investigations were conducted using cyanide as the model analytes.

To understand the thermodynamic properties of the CDA, the Gibbs free energy changes ($\Delta G°$) between M_D and M_A of **1–3** were found and calculated as −30.4, −25.3, and −15.1 kJ·mol^{-1}, respectively (Table 2). The $\Delta G°$ value of the adduct between $Cu^{II}(dien)^{2+}$ and CN^- (−37.9 kJ·mol^{-1}) is more stable relative to those of bimetallic systems **1–3**. By comparing these four $\Delta G°$ values, we predicted that when CN^- is introduced into the bimetallic systems (**1**, **2**, or **3**), it would displace the $Cu^{II}(dien)^{2+}$ unit from its ferrous partner by breaking the cyano-bridges, because the formed $[CN–Cu^{II}(dien)]^+$ adduct is more stable than the

View Article Online
DOI: 10.1039/C6SC05584B

precursor. Figures 2a–c show the evidence of breaking the cyano-bridges of complexes **1–3** by showing the restoration of the spectroscopic properties of $[Fe^{II}(CN)_6]^{4-}$, $[Fe^{II}(t\text{Bubpy})(CN)_4]^{2-}$, and $Fe^{II}(t\text{Bubpy})_2(CN)_2$ upon the addition of cyanide to **1–3**, respectively. Most importantly, through cleaving the cyano-bridges upon the addition of cyanide to **1–3**, the corresponding displaced Cu^{II}-complex $[Cu^{II}(\text{dien})(CN)]^+$ (*m/z* 192.0 $[M]^+$) was found and identified by ESI-MS spectroscopic analysis (Figure S4a).

We believe that the displacement of the Cu^{II}-complex (through bridge cleavage by the target analyte) from the bimetallic systems is not only controlled by the abovementioned thermodynamic factors, but also that the different displacement kinetics of the systems could provide "smart" deactivation-activation functions which would enable us to establish a CDA system. To prove this concept, kinetic studies were conducted on the rates of cyano-bridge cleavage between the Fe^{II} and Cu^{II} metal centers in the bimetallic systems by cyanide. Figure 3 shows that the rate constants for cyano-bridge cleavage in **1–3** by cyanide were determined to be 18.8, 32.0, and 58.3 $M^{-1}\cdot s^{-1}$, respectively. The results indicate that complex **3** is the fastest to release the Cu-catalyst for the oxidation reaction. The rates of cyanate formation with **1–3** were found increased with respect to their decreasing ΔG^0 (**1–3** = −30.4, −25.3 and −15.1 $kJ\cdot mol^{-1}$, respectively) and also in line with the rate constants for cyano-bridge cleavage of **1–3** by cyanide ion (18.8, 32.0, and 58.3 $M^{-1}\cdot s^{-1}$ Figure 3). The rate constant of cyanate formation from the oxidation of cyanide with H_2O_2 as the oxidant under the catalytic action of Cu^{II} was reported as 249.5 $M^{-1}\cdot s^{-1}$ (Figure S5).[21] The results reveal that the cleavage of the cyano-bridge between the metallic donor and acceptor to release the Cu^{II} complex (Scheme 2: 1st step of the overall CDA process) is the rate determining step, whereas the 2nd step of the process, the catalytic oxidation of cyanide, is faster.

View Article Online
DOI: 10.1039/C6SC05584B

Threshold-controlled catalytic properties of the CDA system.

For the investigation of the smart threshold-controlled properties of the CDA, the initial test solutions containing cyanide, H_2O_2, and **1**, **2** or **3** in a molar ratio of 10:65:1 in buffered aqueous DMF solution were prepared for the analyses. The concentrations of CN^- and NCO^- in the test solutions were measured under ambient conditions.[17,20d] Figure 4a shows that all the complexes could catalyze the oxidation of cyanide to cyanate quantitatively within 150 min with H_2O_2 as the oxidant. Control experiments in the absence of the complexes or H_2O_2 revealed that no cyanide was oxidized to cyanate throughout the period. On the other hand, in the reaction using $Cu^{II}(dien)Cl_2$ instead of the bimetallic complexes under the same conditions, cyanide was quantitatively oxidized to cyanate. This confirmed that the Cu^{II}-complex is the active catalyst in the oxidation reaction.

From the thermodynamics consideration, all these complexes of **1–3** are able to release the inhibited Cu-catalyst in the presence of cyanide as the $\Delta G°$ value (-37.9 kJ·mol^{-1}) of $Cu^{II}(dien)^{2+}$ and CN^- adduct is much lower than the formation of $[(L)_x(CN)_yFe^{II}$—C≡N—$Cu^{II}(dien)]$ (Table 2). However, Figures 4b–d show the most interesting findings that complexes **1–3** do not exhibit their catalytic properties, even though the reactions are considered thermodynamically feasible, if the cyanide concentration does not reach certain thresholds. However, by taking into account their kinetic properties, the initial cyanide concentration needs to reach thresholds of 0.2, 0.1, and 0.02 mM for **1**, **2**, and **3**, respectively, to break their cyano-bridges and release $[CN\text{-}Cu^{II}(dien)]^+$ to catalyze cyanide oxidation. In addition, we observed obvious plateaus from Figures 4b–d when the oxidation reaction of CN^- proceeding for a certain period of time that the product of NCO^- accumulated in the reaction environment. The plateaus may indicate that the catalytic system is being slow-down and/or an inhibition effect from the negative feedback loop of the product

generated.[2j] A proposed mechanism for the catalytic oxidation of CN^- to NCO^- by the latent catalyst is shown in Scheme 2.

To further demonstrate the scope of the CDA as a general and smart catalytic system, another substrate, oxalate, was also investigated. The $\Delta G°$ value (-39.0 kJ·mol^{-1}) of the adduct between $Cu^{II}(dien)^{2+}$ and $HOOC\text{-}COO^-$ was found to be larger than those of the systems **1–3** (-30.4, -25.3, and -15.1 kJ·mol^{-1}, respectively, Table 2) (Figure S6). Because of this thermodynamic trigger, an off-on control is introduced into the CDA: Figure S7 in the SI shows that, in the presence of **1** under UV-vis irradiation at room temperature, the degradation of the oxalate (3.125×10^{-2} M) to CO_2 is boosted rapidly in the first 150 min and gradually increases afterwards. In addition, the kinetic properties of the systems impart smart properties. Figure S7 also reveals that even though complex **1** could thermodynamically undergo cyano-bridge cleavage in the presence of oxalate to release the Cu^{II} unit (Figure S4b) for the catalytic oxidation of oxalate into CO_2, it does not start the CDA reaction. For example, complex **1** requires that the initial oxalate concentration reaches 1.25×10^{-3} M (the threshold) to cleave the cyano-bridge, release the Cu^{II} unit, and catalyze oxalate oxidation. A proposed mechanism for the catalytic oxidation of oxalate to CO_2 by the latent catalyst is shown in Scheme 2. The CDA system is therefore being smart, playing two consecutive roles of sensing a target pollutant and executing a preset chemical process at a specific concentration level of pollutants.

Degradation of cyanide in real wastewater samples by Catalyst Displacement Assay. After carefully verifying the basic and crucial factors (thermodynamic and kinetic properties) of the CDA, complex **3** was used to test its applicability and "smart" performance in real wastewater treatment. Both domestic and industrial wastewater samples (level I, untreated sewage from a residential area system and sewage from an industrial zone,

View Article Online
DOI: 10.1039/C6SC05584B

respectively) were collected in Hong Kong, China. The samples were filtered through 0.45 μm pore-size membrane filters (Pall Corporation) to remove insoluble substances before examination. The World Health Organization suggests a maximum allowable level of cyanide in wastewater of 20 μM (0.5 $mg \cdot L^{-1}$).[4] The wastewater samples were spiked with 10, 20 or 30 μM cyanide and their degradation/oxidation was analyzed at room temperature with complex **3** in the presence of H_2O_2. (Based on the results described above, complex **3** was able to initiate the oxidation of cyanide at 20 μM.) In the presence of **3**, when the cyanide content of the samples reached 20 μM, the oxidation of cyanide to cyanate was initiated (Table 3; Figure S8). However, it is important to note that while the cyanide content of the samples set as 10 μM (i.e., less than the threshold concentration), no cyanide was oxidized to cyanate throughout the period. Control experiments in the absence of the complex revealed that no cyanide was oxidized. These results indicate that the smart-functioning CDA concept is applicable, even in the presence of organic/inorganic matters in actual domestic and industrial wastewater samples.

Conclusion

Three bimetallic complexes were synthesized using a supramolecular approach with different metallic donors, $[Fe^{II}(CN)_6]^{4-}$, $[Fe^{II}(t\text{Bubpy})(CN)_4]^{2-}$, and $Fe^{II}(t\text{Bubpy})_2(CN)_2$, to bridge with a metallic acceptor, $[Cu^{II}(dien)]^{2+}$, through a cyano-bridge as latent catalysts. The study of their thermodynamic and kinetic properties provided insight on how to establish a smart off-on sensing and threshold-controlled latent catalytic system for degradation of toxic pollutants. With this "smart" deactivation-activation function for controlling targeted reactions, the catalyst displacement assay (CDA) system could be used for on-site applications such as wastewater treatment with a pre-set threshold for the elimination of cyanide from reservoirs.

View Article Online
DOI: 10.1039/C6SC05584B

Acknowledgements

The work described in this paper was funded by a grant from The Education University of Hong Kong (Project No. R3444, R4175 and R4201), and grants from the Research Grants Council of Hong Kong SAR, China (ECS No. 800312 and GRF 18300415).

View Article Online
DOI: 10.1039/C6SC05584B

References

1. (a) Trnka, T. M.; Grubbs, R. H. The development of L_2X_2Ru = CHR olefin metathesis catalysts: An organometallic success story. *Acc. Chem. Soc.* **2001**, *34*, 18-29; (b) Lee, J.; Farha, O. K.; Roberts, J.; Scheidt, K. A.; Nguyen, S. T.; Hupp, J. T. Metal-organic framework materials as catalysts. *Chem. Soc. Rev.* **2009**, *38*, 1450-1459; (c) Britovsek, G. J. P.; Gibson, V. C.; Wass, D. F. The search for new-generation olefin polymerization catalysts: Life beyond metallocenes. *Angew. Chem. Int. Ed.* **1999**, *38*, 428-447; (d) Noyori, R. Asymmetric catalysis: Science and opportunities (Nobel lecture). *Angew. Chem. Int. Ed.* **2002**, *41*, 2008-2022.

2. (a) Li, S. J.; Ge, Y.; Tiwari, A; Wang, S. Q.; Turner, A. P. F.; Piletsky, S. A. 'On/off'-switchable catalysis by a smart enzyme-like imprinted polymer. *J. Catal.* **2011**, *278*, 173-180; (b) Piermattei, A.; Karthikeyan, S.; Sijbesma, R. Activing catalysts with mechanical force. *Nat. Chem.* **2009**, *1*, 133-137; (c) Groote, R.; Jakobs, R. T. M.; Sijbesma, R. P. Mechanocatalysis: forcing latent catalysts into action. *Polym. Chem.* **2013**, *4*, 4846-4859; (d) Blanco, V.; Leigh, D. A.; Marcos, V. *Chem. Soc .Rev.* **2015**, *44*, 5341-5370; (e) Sinn, H.; Kaminsky, W.; Vollmer, H. J.; Woldt R. Living polymers on polymerization with extremely productive Ziegler catalysts. *Angew. Chem. Int. Ed.* **1980**, *19*, 390–392; (f) Slugovc, C.; Burtscher, D.; Stelzer, F.; Mereiter K. Thermally switchable olefin metathesis initiators bearing chelating carbenes: Influence of the chelate's ring size. *Organometallics* **2005**, *24*, 2255–2258; (g) Slaugh, L. H; Mullineaux, R. D. Novel hydroformylation catalysts. *J. Organomet. Chem.* **1968**, *13*, 469–477; (h) Sentman, A. C.; Csihony, S.; Waymouth, R. M.; Hedrick, J. L. Silver (I)–carbine complexes/ionic liquids: Novel N-heterocyclic carbene delivery agents for organocatalytic transformations. *J. Org. Chem.* **2005**, *70*, 2391–2393; (i) Gawin, R.; Makal, A.; Wozniak, K.; Mauduit, M.; Grela, K. A dormant ruthenium catalyst bearing a chelating carboxylate ligand: In situ activation and application in metathesis reactions.

Angew. Chem. Int. Ed. **2007**, *46*, 7206–7209; (j) Pramanik, S.; Aprahamian, I. Hydrazone Switch-Based Negative Feedback Loop. *J. Am. Chem. Soc.* **2016**, *138*, 15142−15145; (k) Zhao, D.; Neubauer, T. M.; Feringa, B. L. *Nat. Commun.*, **2015**, *6*, 6652; (l) Vlatkovic, M.; Collins, B. S. L.; Feringa, B. L. *Chem. Eur. J.*, **2016**, *22*, 17080.

3. (a) Pati, P. B. Organic chemodosimeter for cyanide: A nucleophilic approach. *Sens. Actuator B-Chem.* **2016**, *222*, 374; (b) Young, C.; Tidwell, L.; Anderson, C. *Cyanide: Social, Industrial, and Economic Aspects*, Mineral, Metals, and Materials Society, Warrendale, **2001**; (c) Wang, F.; Wang, L.; Chen, X. Q.; Yoon, J. Y. Recent progress in the development of fluorometric and colorimetric chemosensors for detection of cyanide ions. *Chem. Soc. Rev.*, **2014**, *43*, 4312-4324; (d) Xu, Z.; Chen, X.; Kim, H. N.; Yoon, J. *Chem. Soc. Rev.*, **2010**, *39*, 127-137; (e) Dash, R. R.; Gaur, A.; Balomajumder, C. Cyanide in industrial wastewaters and its removal: A review on biotreatment. *J. Hazard. Mater.* **2009**, *163*, 1-11.
4. Shan, D.; Mousty, C.; Cosnier, S. *Anal. Chem.* **2004**, *76*, 178.
5. (a) Marugan, J.; van Grieken, R.; Cassano, A. E.; Alfano, O. M. Scaling-up of slurry reactors for the photocatalytic oxidation of cyanide with TiO_2 and silica-supported TiO_2 suspensions. *Catal. Today* **2009**, *144*, 87-93; (b) Frank, S. N.; Bard, A. J. Heterogeneous photocatalytic oxidation of cyanide ion in aqueous-solutions at TiO_2 powder *J. Am. Chem. Soc.* **1977**, *99*, 303-304.
6. (a) Sarla, M.; Pandit, M.; Tyagi, D. K.; Kapoor, J. C. Oxidation of cyanide in aqueous solution by chemical and photochemical process. *J. Hazard. Mater.* **2004**, *116*, 49-56; (b) Chen, F. Y. ; Zhao, X.; Liu, H. J.; Qu, J. H. Reaction of Cu(CN)(3)(2-) with H_2O_2 in water under alkaline conditions: Cyanide oxidation, Cu+/Cu2+ catalysis and H_2O_2 decomposition. *Appl. Catal. B-Environ.* **2014**, *158*, 85-90; (c) Christoskova, St.; Stoyanova, M. *J. Hazard. Mater.* **2009**, *165*, 690-695.

7. (a) Li, Q.; Cai, Y.; Yao, H.; Lin, Q.; Zhu, Y. R.; Li, H.; Zhang, Y. M.; Wei, T. B. *Spectrochimica Acta Part A: Molecular and Biomolecular Spectroscopy* **2015**, *136*, 1047; (b) Xu, Y.; Dai, X.; Zhao, B. X. *Spectrochimica Acta Part A: Molecular and Biomolecular Spectroscopy* **2015**, *138*, 164; (c) Misra, R.; Jadhav, T.; Dhokale, B.; Mobin, S. M. *Dalton Trans.* **2015**, *44*, 16052; (d) references cited in [21]; (e) Khajehsharifi, H.; Bordbar, M. M. *Sensors and Actuators B* **2015**, *209,* 1015; (f) Heying, R. S.; Nandi, L. G.; Bortoluzzi, A. J.; Machado, V. G. *Spectrochimica Acta Part A: Molecular and Biomolecular Spectroscopy* **2015**, *136*, 1491; (g) Tang, L.; Cai, M. *Sensors and Actuators B* **2012,** *173*, 862; (h) Feng, L.; Li, H.; Li, X.; Chen, L.; Shen, Z.; Guan, Y. *Anal. Chim. Acta* **2012**, *743*, 1; (i) Jose, D. A.; Elstner, M.; Schiller, A. *Eur. J Chem.* **2013**, *19*, 14451-14457; (j) references cited in Lou, X.; Ou, D.; Li, Q.; Li, Z. *Chem. Commun.* **2012**, *48*, 8462-8477.

8. Lavigne, J. L.; Anslyn, E. V. *Angew. Chem. Int. Ed.* **1999**, *38*, 3666; (b) Wiskur, S. L.; Anslyn, E. V. *J. Am. Chem. Soc.* **2001**, *123*, 10109; (c) Alt-Haddou, H.; Wiskur, S. L.; Lynch, V. M.; Anslyn, E. V. *J. Am. Chem. Soc.* **2001**, *123*, 11296; (d) Schneider, S. E.; O'Neil, S. N.; Anslyn, E. V. *J. Am. Chem. Soc.* **2000**, *122*, 542; (e) Zhong, Z.; Anslyn, E. V. *J. Am. Chem. Soc.* **2002**, *124*, 9014; (f) Wiskur, S. L.; Ait-Haddou, H.; Lavigne, J. J.; Anslyn, E. V. *Acc. Chem. Res.* **2001**, *34*, 963; (g) Nguyen B. T.; Anslyn, E. V. *Coord. Chem. Rev.* **2006**, *250*, 3118; (k) Anslyn, E. V. *J. Org. Chem.* **2007**, *72*, 687.

9. Fabbrizzi, L.; Leone, A.; Taglietti, A. *Angew Chem. Int. Ed.* **2001**, *40*, 3066; (b) Fabbrizzi, L.; Foti, F.; Taglietti, A. *Org. Lett.* **2005**, *7*, 2603; (c) Hortala, M. A.; Fabbrizzi, L.; Marcotte, N.; Stomeo, F.; Taglietti, A. *J. Am. Chem. Soc.* **2003**, *125*, 20; (d) Amendola, V.; Bergamaschi, G.; Buttafava, A.; Fabbrizzi, L.; Monzani, E. *J. Am. Chem. Soc.* **2010**, *132*, 147.

10. Jimenez, D.; Martinez-Manez, R.; Sancenon, F.; Ros-Lis, J. V.; Benito, A.; Soto, J.; *J. Am. Chem. Soc.* **2003**, *125*, 9000; (b) Comes, M.; Rodriguez-Lopez, G.; Marcos, M. D.;

Martinez-Manez, R; Sancenon, F.; Soto, J.; Villaescusa, L. A.; Amoros, P.; Beltran, D. *Angew. Chem. Int. Ed.* **2005**, *44*, 2918; (c) Martinez-Manez, R; Sancenon, F. *Chem. Rev.* **2003**, *103*, 4419; (d) Martinez-Manez, R; Sancenon, F.; Biyikal, M.; Hecht, M.; Rurack, K. *J. Mater. Chem.* **2011**, *21*, 12588; (e) Moragues M, E.; Martinez-Manez, R.; Sancenon, F. *Chem. Soc. Rev.* **2011**, *40*, 2593.

11. (a) Chow, C. F.; Lam, M. H. W.; Wong, W. Y. *Dalton Transactions* **2005**, *3*, 475-484; (b) Chow, C. F.; Lam, M. H. W.; Wong, W. Y. *Inorg. Chem.* **2004**, *43*, 8387; (c) Koo, C. K.; Chow, C. F.; Chiu, B .K. W.; Lam, M. H. W.; Wong, W. Y. *Eur. J. Inorg. Chem.* **2008**, 1318; (d) Chow, C. F.; Lam, M. H. W.; Wong, W. Y. *Anal. Chem.* **2013**, *85*, 8246; (e) Chow, C. F.; Ho, Y. F.; Gong, C. B. *Anal. Chem.* **2015**, *87*, 6112−6118.
12. Krause, R. A. *Inorg. Chim. Acta* **1977**, *22*, 209–213.
13. Schilt, A. A. *J. Am. Chem. Soc.* **1960**, *82*, 3000.
14. Trendafilova, N.; Nikolov, G. S.; Bauer, G.; Kellner, R. *Inorg. Chim. Acta* **1993**, *210*, 77.
15. Connors, K. A. *Binding Constants, The Measurement of Molecular Complexes Stability*, John Wiley and Sons, New York, **1987**.
16. Hubaux, A.; Vos, G. *Anal. Chem*. **1970**, *42*, 849–855.
17. Erman, J. E. *Biochem.* **1974**, *13*, 39–44.
18. (a) Chow, C. F.; Ho, P. Y.; Wong, W. L.; Gong, C. B. *Chem. Eur. J.* **2015**, *21*, 12984–12990; (b) Chow, C. F.; Ho, P. Y.; Gong, C. B. *Analyst*, **2014**, *139*, 4256.
19. Keene, T. D.; Komm, T.; Hauser, J.; Kramer K. W. *Inorg. Chim. Acta* **2011**, *373*, 100–106.
20. (a) Beattie, J. K.; Polyblank, G. A. *Aust. J. Chem.* **1995**, *48*, 861–868; (b) Sarla, M.; Pandit, M.; Tyagi, D. K.; Kapoor, J. C.; *J. Hazad. Mater.* **2004**, *B116*, 49–56; (c) Acheampong, M. A.; Meulepas, R. J. W.; Lens, P. N. L. *J. Chem. Technol. Biotechnol.*

DOI: 10.1039/C6SC05584B

2010, *85*, 590–613; (d) Garcia, V.; Hayrynen, P.; Landaburu-Aguirre, J.; Pirila, M.; Keiski, R. L.; Urtiaga, A. *J. Chem. Technol. Biotechnol.* **2014**, *89*, 803–813.

21. Sarla, M.; Pandit, M.; Tyagi, D. K.; Kapoor, J. C. *J. Hazard. Mater.* **2004**, *B116*, 49-56.

View Article Online
DOI: 10.1039/C6SC05584B

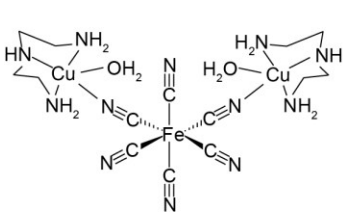

Complex **1**

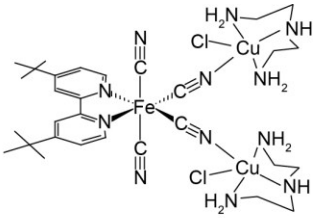

Complex **2**

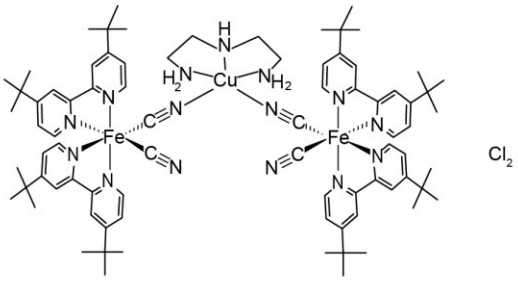

Complex **3**

Scheme 1. Bimetallic complexes **1–3** used as the CDA systems

View Article Online
DOI: 10.1039/C6SC05584B

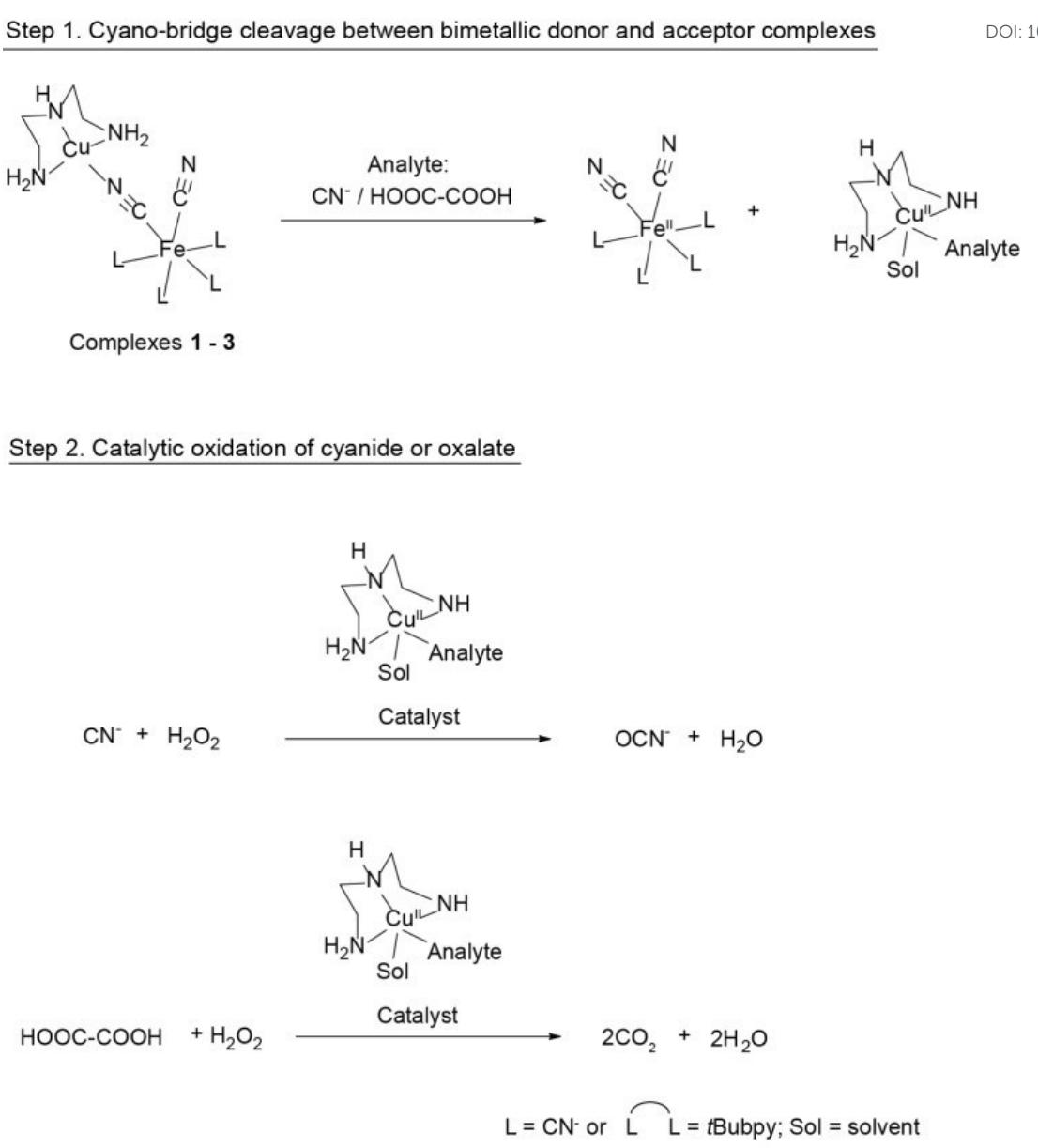

Scheme 2. Proposed mechanism for the overall CDA process. The release of the active catalyst is triggered by cyanide/oxalate in solution, which then catalyzes the oxidation of free cyanide/oxalate to the products cyanate/carbon dioxide, respectively. The development of the colored solution from the $Fe(CN)_2(L)_4$ complex indicates the reaction has taken place.

View Article Online
DOI: 10.1039/C6SC05584B

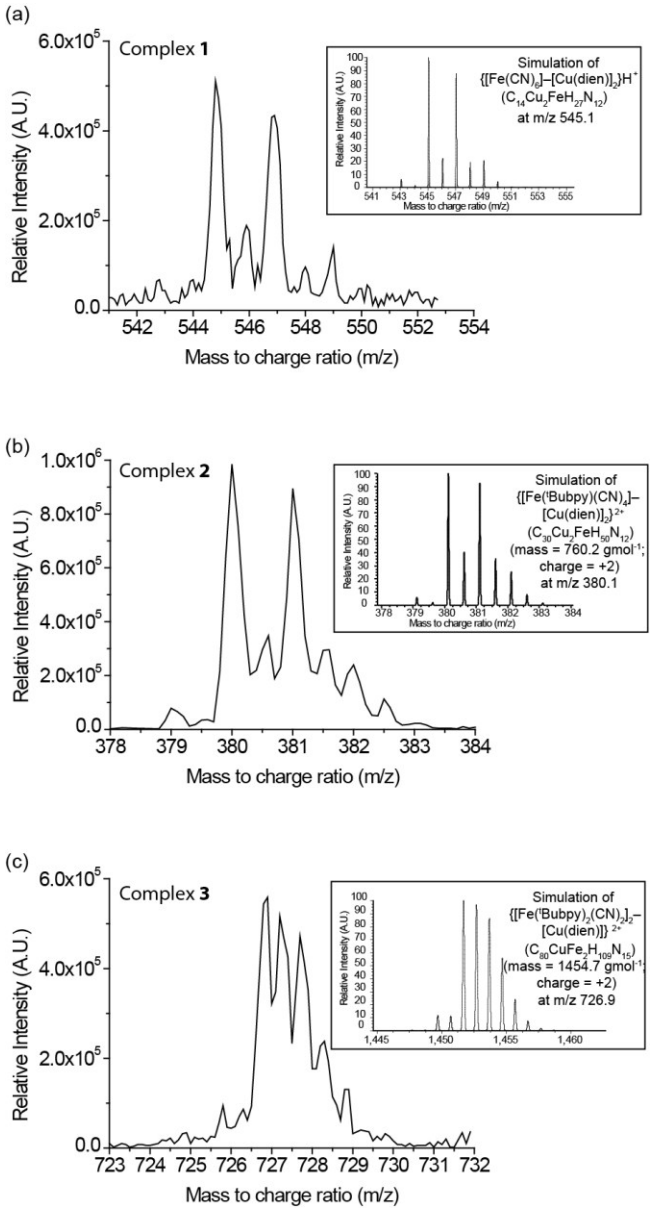

Figure 1. ESI-MS spectra of the isotopic distribution of (a) complex **1**, (b) complex **2**, and (c) complex **3**: and *(inset)* simulations based on their molecular formulas. All the experiments were conducted in DI water/methanol.

View Article Online
DOI: 10.1039/C6SC05584B

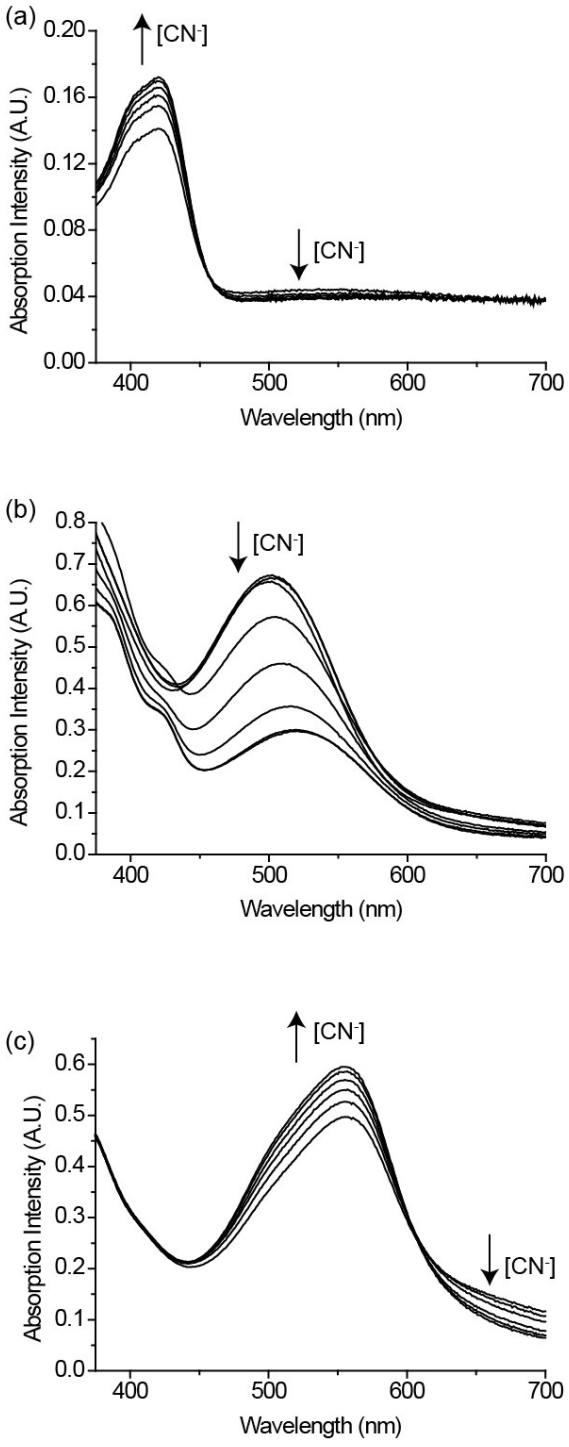

Figure 2. UV-vis spectroscopic titration curves of (a) **1**, (b) **2**, and (c) **3** with CN^-. Addition of cyanide anions to **1–3** restored the characteristic spectroscopic properties of $[Fe^{II}(CN)_6]^{4-}$, $[Fe^{II}(t\text{Bubpy})(CN)_4]^{2-}$, and $Fe^{II}(t\text{Bubpy})_2(CN)_2$, respectively. All the titrations were examined in aqueous DMF (1:1 v/v, 1.50 mL aqueous HEPES buffer at pH 7.4 + 1.50 mL DMF) at 298 K with complex concentrations of 1×10^{-4} M and CN^- concentrations from 0 to 2.0×10^{-4} M.

View Article Online
DOI: 10.1039/C6SC05584B

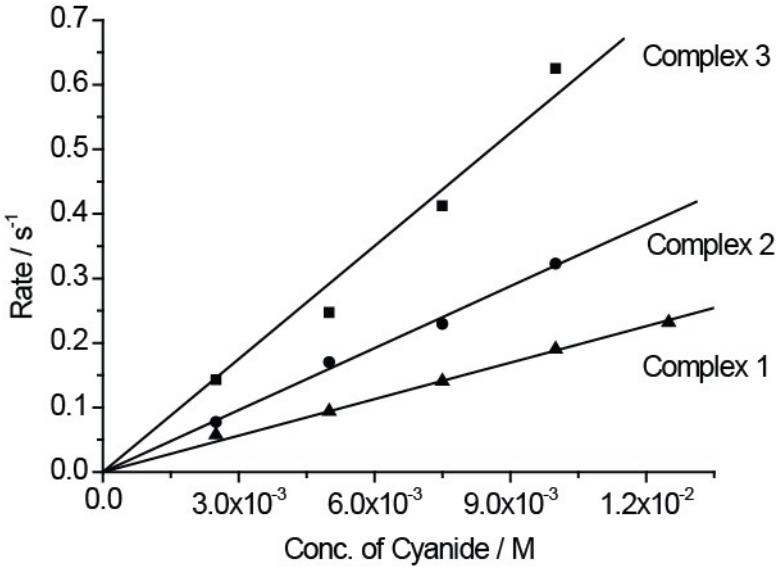

Figure 3. Kinetic plots of the apparent association rate constant k_{obs} (s^{-1}) versus cyanide concentration. The rate constant values were calculated from the slopes of the curves ($y = mx$; **1** = 18.8 $M^{-1}s^{-1}$; **2** = 32.0 $M^{-1}s^{-1}$; and **3** = 58.3 $M^{-1}s^{-1}$).

View Article Online
DOI: 10.1039/C6SC05584B

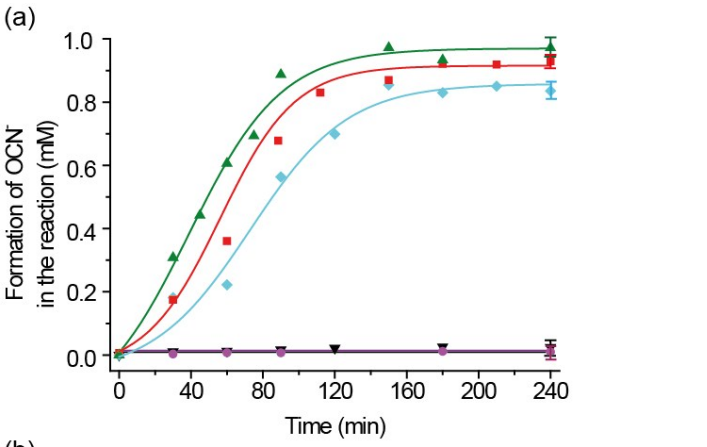

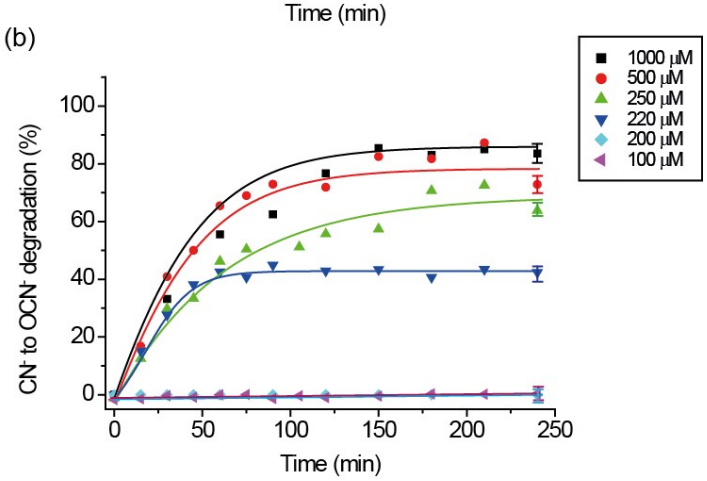

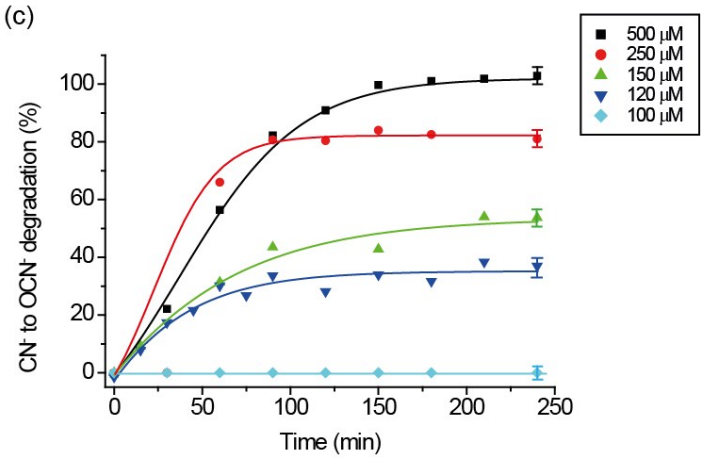

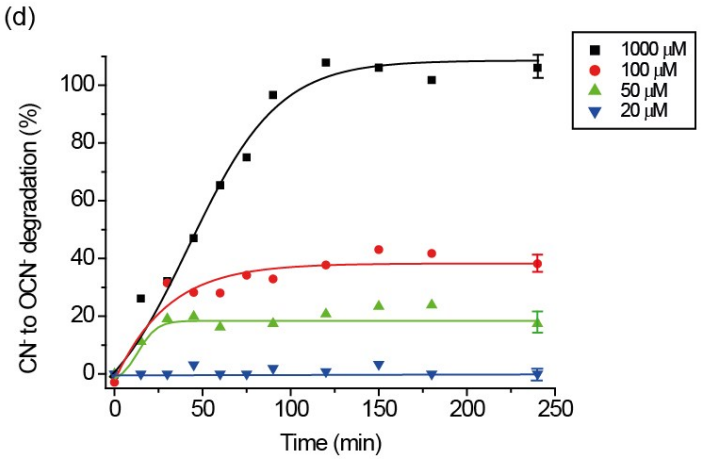

View Article Online
DOI: 10.1039/C6SC05584B

Figure 4. (a) Formation of cyanate from the oxidation of cyanide (1 mM) in the presence of **1** (◆), **2** (■), and **3** (▲) against time. The formation of cyanate in the absence of H_2O_2 (●) or catalyst (▼) concentration. All the experiments were performed with a 10:65:1 molar ratio of cyanide, H_2O_2, and the "$Cu^{II}(dien)^{2+}$" of **1**, **2**, or **3** at room temperature under ambient atmosphere. Formation of cyanate in the presence of (b) **1**, (c) **2**, and (d) **3** with respect to different initial concentrations of cyanide versus time. All the experiments were performed with a 65:2 molar ratio of H_2O_2 (6.53 mM) and the "$Cu^{II}(dien)^{2+}$" of **1**, **2**, or **3** at room temperature under ambient atmosphere. Error bar is the mean value of three independent experiments.

View Article Online
DOI: 10.1039/C6SC05584B

Table 1. IR spectroscopic study of the cyano-stretching frequencies ($\nu_{C\equiv N}$) of complexes **1–3** and their precursor complexes

Entry	Complexes	$\nu_{C\equiv N}$ (cm^{-1})
1	$[Fe^{II}(CN)_6]$–$[Cu^{II}(dien)]_2$ **(1)**	2039, 2047, 2103
2	$[Fe^{II}(^tBubpy)(CN)_4]$–$[Cu^{II}(dien)Cl]_2$ **(2)**	2059, 2084, 2103, 2114
3	$\{[Fe^{II}(^tBubpy)_2(CN)_2]_2$–$[Cu^{II}(dien)]\}Cl_2$ **(3)**	2068, 2082
4	$K_4[Fe^{II}(CN)_6]$	2030, 2043
5	$K_2[Fe^{II}(^tBubpy)(CN)_4]$	2053, 2067, 2085
6	$Fe^{II}(^tBubpy)_2(CN)_2$	2080

Table 2. Binding constants (log *K*) and Gibbs free energy changes (ΔG^0) for the complexation of cyanide anion and different Fe^{II} species to the $[Cu^{II}(dien)]^{2+}$ complex

	Acceptor	Donor	log *K* [a]	ΔG^0 [a] / kJmol^{-1}
1	$[Cu^{II}(dien)Cl_2]$	Oxalate (HOOC-COO^-)	6.84	-39.0
2	$[Cu^{II}(dien)(ClO_4)](ClO_4)$	CN^-	6.64[b]	-37.9[b]
3	$[Cu^{II}(dien)Cl_2]$	$K_4[Fe^{II}(CN)_6]$	5.32	-30.4
4	$[Cu^{II}(dien)\ Cl_2]$	$K_2[Fe^{II}(^tBubpy)(CN)_4]$	4.44	-25.3
5	$[Cu^{II}(dien)Cl_2]$	$Fe^{II}(^tBubpy)_2(CN)_2$	2.65	-15.1

[a]Binding strengths were measured by UV spectroscopic titration and calculated using the Benesi-Hildebrand equations. Except entry 1, which was performed in aqueous phosphate buffer at pH 4, all reactions were performed in aqueous DMF (1:1 v/v, 1.50 mL aqueous HEPES buffer at pH 7.4 + 1.50 mL DMF) at 298 K. [b]log *K* and ΔG^0 data are cited from reference [11b and 18a].

View Article Online
DOI: 10.1039/C6SC05584B

Table 3 Results of cyanide degradation by **3** in domestic (level I, untreated) and industrial wastewater samples

Wastewater samples	Cyanide added (μM)	Cyanate generated (μM)	Conversion after 4 h (%)
Domestic (level I, untreated)	10	0	0
	20	6.1	40.4
	30	12.9	42.9
Industrial	10	0	0
	20	6.6	33.1
	30	14.8	49.4